BMC Medical Imaging

RESEARCH Open Access

Diagnostic performance of ultrasound elastography in differentiating malignant from benign breast microcalcifications: a case-control study

Jing Yan[1,3*] and Sisi Fang[2]

Abstract

Objective To evaluate the sensitivity and specificity of ultrasound elastography in differentiating between malignant and benign breast microcalcifications through a case-control study.

Methods A total of 300 female patients were enrolled in this study, equally divided between malignant ($n=150$) and benign ($n=150$) microcalcification groups. The malignant cases were histologically confirmed as ductal carcinoma in situ or invasive breast cancer, while benign cases were confirmed through histology or follow-up as fibroadenoma, fibrocystic changes, or benign calcifications. Ultrasound elastography parameters, including elastic modulus (kPa), strain ratio, and elasticity scores, were measured and compared between groups. Multiple logistic regression analysis was performed to identify independent predictors, and diagnostic performance was evaluated using ROC curve analysis.

Results Malignant lesions demonstrated significantly higher mean elasticity values compared to benign lesions (88.3 ± 16.2 kPa vs. 45.7 ± 9.8 kPa, $P<0.001$). The strain ratio and elasticity scores were also significantly elevated in the malignant group (both $P<0.001$). Multivariate analysis identified elastic modulus (OR = 1.09, 95%CI: 1.06–1.12, $P<0.001$) and strain ratio (OR = 2.50, 95%CI: 1.70–3.80, $P<0.001$) as independent predictors of malignancy. Using an optimal cutoff value of 62 kPa for elasticity, the diagnostic sensitivity was 88.0% (95%CI: 81.5-92.8%) and specificity was 86.7% (95%CI: 79.5-91.9%), with an accuracy of 89.0%. The area under the ROC curve (AUC) for elasticity alone was 0.95 (95%CI: 0.92–0.98), which improved to 0.97 (95%CI: 0.94–0.99) when combined with strain ratio ($P=0.018$). High interobserver agreement was demonstrated (Kappa = 0.84, 95%CI: 0.79–0.88), and Bland-Altman analysis confirmed excellent measurement reliability.

Conclusion Ultrasound elastography demonstrates high diagnostic accuracy in differentiating between malignant and benign breast microcalcifications, with excellent reproducibility and reliability. The combination of elasticity values and strain ratio provides superior diagnostic performance compared to single parameters alone, suggesting its potential as a valuable tool in clinical practice for the evaluation of breast microcalcifications.

*Correspondence:
Jing Yan
185706865551@163.com

Full list of author information is available at the end of the article

Keywords Breast microcalcifications, Ultrasound elastography, Elasticity imaging, Breast cancer, Diagnostic accuracy

Introduction

Breast cancer remains one of the most prevalent malignancies affecting women worldwide, with microcalcifications being a crucial early diagnostic indicator detected in approximately 30–50% of mammographically identified breast lesions [1]. The accurate differentiation between malignant and benign microcalcifications represents a significant clinical challenge, as these tiny calcium deposits can be the earliest visible sign of breast cancer, particularly ductal carcinoma in situ (DCIS) [2].

Traditional imaging methods, including mammography and conventional ultrasound, while valuable in detecting microcalcifications, have shown limitations in definitively characterizing their nature. Mammography, despite its high sensitivity in detecting calcifications, often demonstrates restricted specificity in distinguishing between benign and malignant lesions, leading to unnecessary biopsies [3]. Recent studies have reported that approximately 70–80% of breast biopsies performed for suspicious microcalcifications ultimately reveal benign pathology, highlighting the need for more accurate diagnostic tools [4]. Ultrasound elastography has emerged as a promising imaging technique that provides information about tissue stiffness, which often correlates with malignancy. This technology has shown considerable potential in various aspects of breast imaging, particularly in the characterization of solid masses [5]. The underlying principle relies on the fact that malignant tissues typically exhibit higher stiffness compared to benign tissues due to increased cellularity and desmoplastic reaction [6]. Recent technological advances have enabled the application of elastography in evaluating microcalcifications, offering both qualitative and quantitative assessments of tissue elasticity [7].

Several studies have demonstrated the value of shear wave elastography in improving the diagnostic accuracy of breast lesions, reporting sensitivity rates ranging from 85 to 95% and specificity rates of 80–90% [8]. However, the specific utility of elastography in evaluating breast microcalcifications has been less extensively studied, with existing research showing varying results [9]. The integration of elastography parameters with conventional imaging features has suggested potential improvements in diagnostic accuracy, particularly in cases where traditional imaging findings are equivocal [10]. Recent technological developments in elastography have introduced more sophisticated quantitative parameters, including elastic modulus measurements and strain ratios, which may provide more objective criteria for lesion characterization [11]. Additionally, advances in machine learning and artificial intelligence have opened new possibilities for integrating multiple elastographic parameters to enhance diagnostic accuracy [12]. The standardization of elastography techniques and interpretation criteria has also progressed, although challenges remain in establishing universally accepted diagnostic thresholds [13]. The potential impact of accurate non-invasive characterization of breast microcalcifications extends beyond diagnostic accuracy. Improved specificity in identifying truly suspicious calcifications could significantly reduce unnecessary biopsies, thereby decreasing healthcare costs and patient anxiety [14]. Furthermore, early accurate identification of malignant calcifications could lead to more timely intervention and potentially improved outcomes [15].

In this study, we aim to evaluate the sensitivity and specificity of ultrasound elastography in differentiating between malignant and benign breast microcalcifications through a case-control evaluation. We additionally provide morphological features, ACR BI-RADS category distributions, and illustrative figures showcasing the various microcalcification patterns and their corresponding elastography findings.

Method

Study design and participants

This prospective case-control study was conducted at the Department of Breast Imaging, Hunan Provincial People's Hospital between January 2022 and December 2023. The study protocol was approved by the institutional review board (IRB number: HN-CS-2023-035), and written informed consent was obtained from all participants. The study was conducted in accordance with the Declaration of Helsinki.

Patient recruitment was conducted through the breast imaging center's routine clinical practice. All consecutive female patients presenting with mammographically detected microcalcifications were screened for eligibility. Inclusion criteria consisted of: (1) female patients aged 18 years or older; (2) presence of breast microcalcifications detected on mammography with BI-RADS categories 3–5; (3) lesion size between 3 and 15 mm; (4) availability of histopathological confirmation or minimum 12-month imaging follow-up for benign cases. Exclusion criteria included: (1) previous breast surgery or biopsy at the site of microcalcifications; (2) ongoing or previous neoadjuvant chemotherapy; (3) breast implants; (4) pregnancy or lactation; (5) technically inadequate elastography images due to poor acoustic window or patient factors.

Imaging protocol and data acquisition

All ultrasound examinations were performed using a high-end ultrasound system (Supersonic Imagine Aixplorer, Aix-en-Provence, France) equipped with a linear array transducer (SL15-4, frequency range: 4–15 MHz). Patients were positioned supine with the ipsilateral arm raised above the head. Conventional B-mode ultrasound was initially performed to locate the microcalcification area corresponding to mammographic findings, using mammographic images for guidance. The scanning parameters were standardized with a frequency of 12 MHz, focal zone set at the level of the lesion, and dynamic range of 50 dB.

The elastography examination was conducted following a standardized protocol developed through consensus among participating radiologists. The room temperature was maintained between 22 and 24 °C to ensure consistent tissue elasticity measurements. For elastography measurements, minimal precompression was applied (pressure indicator level 2–3) to avoid artificial tissue stiffening. The region of interest (ROI) was set to include both the microcalcification area and surrounding normal tissue, with a minimum margin of 5 mm around the target lesion. The imaging plane was oriented perpendicular to the chest wall, and patients were instructed to hold their breath for 3–5 s during each acquisition.

Three independent measurements were obtained for each lesion, with a minimum 10-second interval between acquisitions to allow tissue recovery. The mean value was used for analysis. The elastography acquisition protocol included both shear wave elastography (SWE) for quantitative measurements and strain elastography for qualitative assessment. For SWE, a standardized ROI size of 2 mm × 2 mm was placed over the stiffest portion of the lesion, as identified by the color mapping. The acquisition time for each measurement was set to 3 s to ensure stable wave propagation.

Image analysis and measurements

Two board-certified radiologists with 10 and 8 years of experience in breast imaging and at least 3 years of experience with elastography independently analyzed the images. Both readers underwent specific training on the study protocol, including calibration sessions with 20 test cases before study initiation. The readers were blinded to the final pathological diagnosis but had access to conventional ultrasound and mammographic images to ensure accurate lesion identification.

For each lesion, comprehensive elastographic parameters were recorded. Quantitative parameters included elastic modulus (kPa) measured at the stiffest portion of the lesion, with both maximum and mean values recorded. Strain ratio was calculated as the ratio of strain in normal adipose tissue at the same depth to that in the lesion area, using standardized ROI placement. The qualitative assessment included a five-point elasticity score based on the color pattern distribution (1: entirely soft, appearing homogeneously green; 2: mostly soft with some blue areas; 3: mixed pattern of blue and green; 4: mostly hard with some green areas; 5: entirely hard, appearing homogeneously blue).

To ensure measurement standardization, specific anatomical landmarks were used for ROI placement, and all measurements were performed at least 3 mm from the skin surface and chest wall to avoid boundary effects. The final measurements for each lesion were determined by averaging the values from both readers. In cases of discrepancy greater than 20% between readers, a consensus was reached through joint review with a third reader with 15 years of experience.

Reference standard

The reference standard for malignant cases was established through histopathological examination of surgical specimens or ultrasound-guided core needle biopsy samples (14-gauge automated needle, minimum of four cores). For benign cases, the reference standard was either histopathological confirmation through biopsy or stability on imaging follow-up for at least 12 months, with follow-up imaging including both mammography and ultrasound. All pathological specimens were reviewed by two experienced breast pathologists (with 12 and 15 years of experience) who were blinded to the elastography findings. Any discrepancies in pathological interpretation were resolved through consensus review.

Statistical analysis

Statistical analyses were performed using SPSS version 26.0 (IBM Corp., Armonk, NY, USA) and R software version 4.1.0 (R Foundation for Statistical Computing, Vienna, Austria). Sample size calculation was based on previous studies, assuming an area under the receiver operating characteristic curve (AUC) of 0.85, with $\alpha = 0.05$ and $\beta = 0.10$, requiring a minimum of 138 cases per group.Continuous variables were expressed as mean ± standard deviation and compared using Student's t-test or Mann-Whitney U test as appropriate after testing for normality using the Kolmogorov-Smirnov test. Categorical variables were presented as frequencies and percentages and compared using Chi-square or Fisher's exact test.Receiver operating characteristic (ROC) curve analysis was performed to evaluate the diagnostic performance of elastography parameters. The optimal cutoff values were determined using the Youden index. Sensitivity, specificity, positive predictive value (PPV), negative predictive value (NPV), and accuracy were calculated with 95% confidence intervals.

Table 1 Comparison of patient, lesion, and microcalcification characteristics ($n = 300$)

Characteristics	Malignant group ($n = 150$)	Benign group ($n = 150$)	*P*-value
Age (years, mean ± SD)	51.3 ± 10.2	49.7 ± 9.8	0.114
Lesion Size (mm, mean ± SD)	7.4 ± 2.1	5.8 ± 1.9	0.015
Breast Density Classification, n (%)	A: 30 (20.0) B: 40 (26.7) C: 50 (33.3) D: 30 (20.0)	A: 38 (25.3) B: 42 (28.0) C: 45 (30.0) D: 25 (16.7)	0.087*
Histological Diagnosis, n (%)	DCIS: 80 (53.3) Invasive Carcinoma: 70 (46.7)	Fibroadenoma: 60 (40.0) Fibrocystic Changes: 50 (33.3) Benign Calcifications: 40 (26.7)	—
ACR BI-RADS Category, n (%)	BI-RADS 3: 20 (13.3) BI-RADS 4: 65 (43.3) BI-RADS 5: 65 (43.3)	BI-RADS 3: 60 (40.0) BI-RADS 4: 70 (46.7) BI-RADS 5: 20 (13.3)	0.001**
Calcification Distribution Pattern, n (%)	Clustered: 72 (48.0) Scattered: 45 (30.0) Sparse punctate: 33 (22.0)	Clustered: 54 (36.0) Scattered: 33 (22.0) Sparse punctate: 63 (42.0)	0.032*

*SD = Standard Deviation; DCIS = Ductal Carcinoma In Situ

*P-value for overall comparison of categorical variables using Chi-square test

**Significant at $P < 0.05$

Multivariate logistic regression analysis was conducted to identify independent predictors of malignancy. Variables with $P < 0.10$ in univariate analysis were included in the multivariate model. The Hosmer-Lemeshow test was used to assess the goodness of fit of the logistic regression model.

Interobserver agreement was evaluated using Cohen's kappa coefficient for categorical variables and intraclass correlation coefficient (ICC) for continuous variables. Bland-Altman analysis was performed to assess the reliability of quantitative measurements. A two-tailed P value < 0.05 was considered statistically significant.

Results

Patient and lesion characteristics

A total of 300 female patients were enrolled in this study, with 150 cases in the malignant microcalcification group (histologically confirmed as ductal carcinoma in situ or invasive breast cancer) and 150 cases in the benign microcalcification group (confirmed through histology or follow-up as fibroadenoma, fibrocystic changes, or benign calcifications). The comparison of clinical and imaging characteristics between the two groups is presented in Table 1(150 malignant, 150 benign).

Table 2 Comparison of elastography parameters between malignant and benign microcalcifications ($n = 300$)

Parameter	Malignant group ($n = 150$)	Benign group ($n = 150$)	*P*-value
Elasticity Value (kPa, mean ± SD)	88.3 ± 16.2	45.7 ± 9.8	< 0.001
Strain Ratio (unitless, mean ± SD)	2.35 ± 0.50	1.15 ± 0.35	< 0.001
Elasticity Score (1–5 points, mean ± SD)	4.2 ± 0.6	2.1 ± 0.7	< 0.001

Note: SD = Standard Deviation; kPa = kilopascals

The malignant group showed slightly larger mean lesion diameters compared to the benign group (7.4 ± 2.1 mm vs. 5.8 ± 1.9 mm, $P = 0.015$). There were no statistically significant differences in mean age ($P = 0.114$) or breast density ($P = 0.087$) between the two groups. The malignant lesions were predominantly BI-RADS 4–5, whereas the benign group had a higher proportion of BI-RADS 3 lesions ($P = 0.001$). Malignant cases included 80 DCIS (53.3%) and 70 invasive carcinomas (46.7%), whereas benign cases were composed of 60 fibroadenomas (40.0%), 50 fibrocystic changes (33.3%), and 40 benign calcifications (26.7%).

Elastography parameter comparison and correlation analysis

The malignant microcalcifications exhibited significantly higher mean elasticity values compared to the benign group (88.3 ± 16.2 kPa vs. 45.7 ± 9.8 kPa, $P < 0.001$). Both strain ratio and semi-quantitative elasticity scores were significantly elevated in the malignant group (both $P < 0.001$). Detailed comparisons of elastography parameters between groups are shown in Table 2.

Spearman correlation analysis revealed a strong positive correlation between elasticity values and strain ratio ($r = 0.75$, $P < 0.001$), and a moderate positive correlation with lesion size ($r = 0.41$, $P < 0.001$). Stratified analysis demonstrated that elasticity values maintained good discriminatory power (AUC > 0.90) in both high breast density (ACR types C and D) and low breast density (ACR types A and B) subgroups.

Illustrative figures of microcalcification patterns

The strain ratios similarly correlated with microcalcification distribution, with the highest values observed in clustered patterns (Fig. 1), intermediate values in scattered patterns (Fig. 2), and lowest values in sparse punctate patterns (Fig. 3). The combination of elasticity values with strain ratios resulted in improved diagnostic accuracy across all distribution patterns, particularly for sparse punctate microcalcifications where the single-parameter performance was relatively lower.

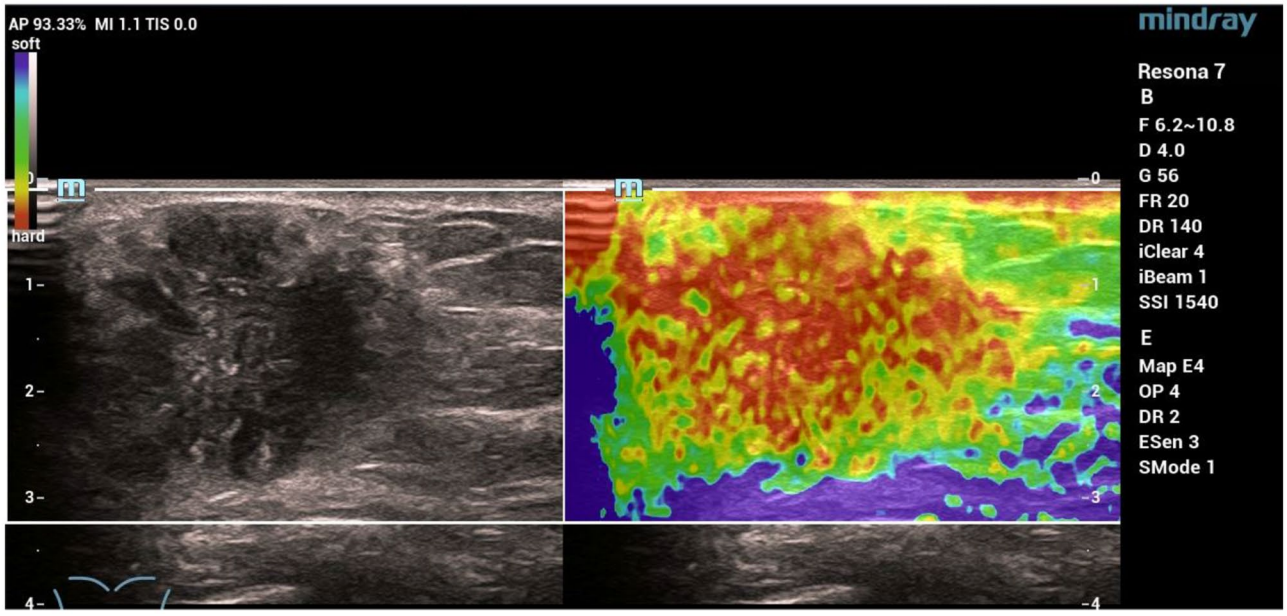

Fig. 1 B-mode ultrasound and elastography imaging of clustered microcalcifications. Representative images from a 54-year-old female patient with clustered microcalcifications (BI-RADS 4). (A) The B-mode ultrasound image (left) shows a hypoechoic area with internal hyperechoic foci corresponding to calcifications. The elastography map (right) demonstrates high stiffness (predominantly red and yellow areas) with a mean elasticity value of 88.3 kPa and strain ratio of 2.35, confirmed as invasive ductal carcinoma on histopathology

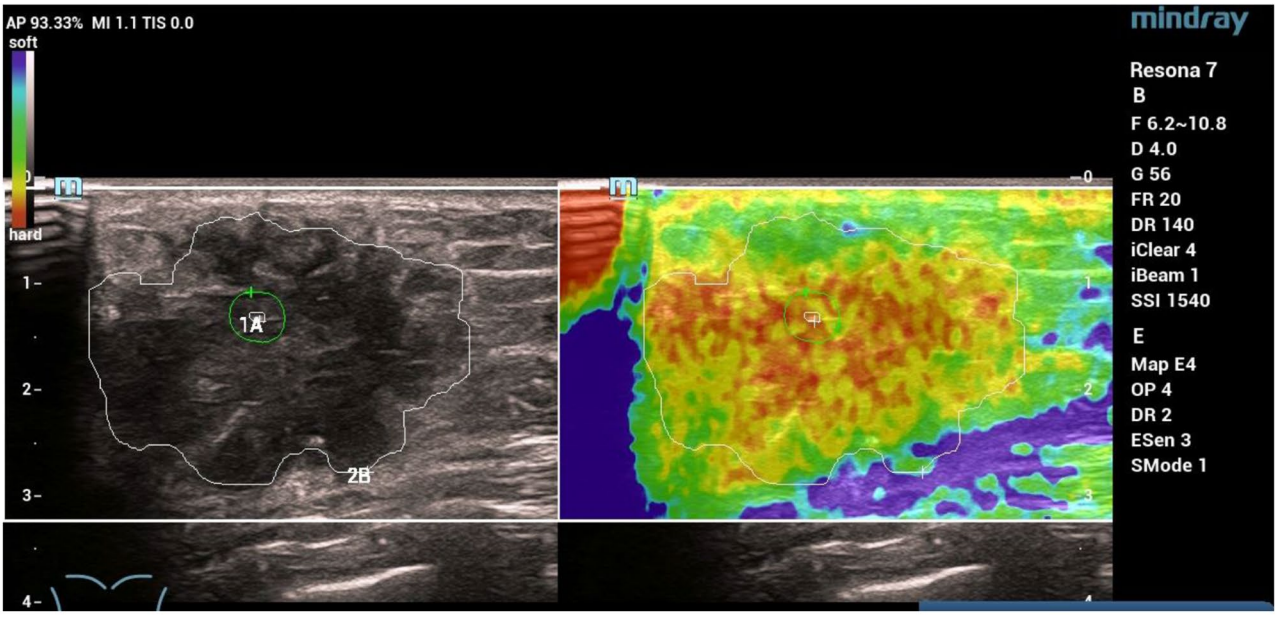

Fig. 2 B-mode ultrasound and elastography imaging of scattered microcalcifications. Representative images from a 49-year-old female patient with scattered microcalcifications (BI-RADS 3). (A) The B-mode ultrasound image (left) shows an isoechoic area with punctate hyperechoic foci (microcalcifications). The elastography map (right) displays a mixed pattern of stiffness (yellow-green predominance) with a mean elasticity value of 45.7 kPa and strain ratio of 1.15, confirmed as fibrocystic changes on histopathology

Multivariate regression analysis and predictive model development

Following multivariate logistic regression analysis incorporating age, lesion size, breast density, elasticity value, and strain ratio, both elasticity value (OR = 1.09, 95%CI: 1.06–1.12, $P < 0.001$) and strain ratio (OR = 2.50, 95%CI: 1.70–3.80, $P < 0.001$) remained independent predictors of malignancy (Table 3). The predictive model constructed using these two independent indicators demonstrated good fit in the Hosmer-Lemeshow test ($P = 0.72$).

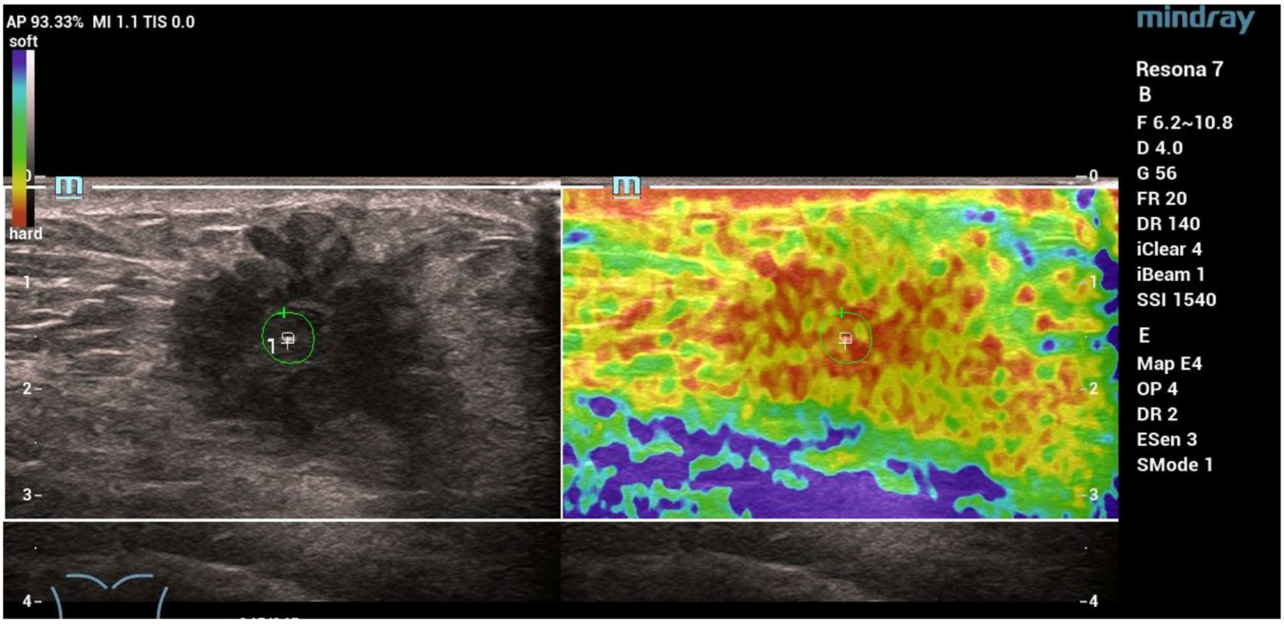

Fig. 3 B-mode ultrasound and elastography imaging of sparse punctate microcalcifications. Representative images from a 51-year-old female patient with sparse punctate microcalcifications (BI-RADS 4). (A) The B-mode ultrasound image (left) demonstrates a heterogeneous area with sparse hyperechoic foci. The corresponding elastography map (right) shows a predominantly softer tissue pattern (green-blue areas) with a mean elasticity value of 48.3 kPa and strain ratio of 1.25, confirmed as benign calcifications on histopathology follow-up

Table 3 Multivariate logistic regression analysis results (Dependent variable: malignant microcalcification = 1, benign Microcalcification = 0)

Variable	OR (95% CI)	*P*-value
Age (years)	1.01 (0.99–1.03)	0.250
Lesion Size (mm)	1.15 (1.05–1.26)	0.003
Breast Density (C, D vs. A, B)	1.20 (0.80–1.80)	0.360
Elasticity Value (kPa)	1.09 (1.06–1.12)	< 0.001
Strain Ratio	2.50 (1.70–3.80)	< 0.001

Note: OR = Odds Ratio; CI = Confidence Interval; kPa = kilopascals

ROC analysis and diagnostic performance evaluation

ROC analysis using elasticity value as an independent indicator identified an optimal cutoff value of 62 kPa. At this threshold, the sensitivity was 88.0% (95%CI: 81.5-92.8%), specificity was 86.7% (95%CI: 79.5-91.9%), with an overall accuracy of 89.0%. The area under the ROC curve (AUC) for the single indicator was 0.95 (95%CI: 0.92–0.98, $P < 0.001$). When strain ratio was incorporated into the model, the AUC improved to 0.97 (95%CI: 0.94–0.99, $P < 0.001$), significantly higher than the single-indicator model (DeLong test, $P = 0.018$) (Fig. 4).

Observer agreement and reproducibility

High interobserver agreement was demonstrated between the two independent readers for elastography image scoring, including elasticity value measurements and strain ratio interpretation (Kappa = 0.84, 95%CI: 0.79–0.88). Bland-Altman analysis showed minimal differences between repeated measurements, with the majority of points falling within ± 2 SD, confirming high measurement reliability (Fig. 5).

Discussion

The accurate differentiation between malignant and benign breast microcalcifications remains a significant clinical challenge in breast imaging. Our study demonstrates that ultrasound elastography provides high diagnostic accuracy in characterizing breast microcalcifications, with the combination of quantitative elasticity values and strain ratios achieving superior diagnostic performance compared to conventional imaging parameters.

The significantly higher elasticity values observed in malignant microcalcifications (88.3 ± 16.2 kPa vs. 45.7 ± 9.8 kPa, $P < 0.001$) align with recent findings in tissue biomechanics research. Recent studies have shown that the increased stiffness in malignant lesions results from complex alterations in the extracellular matrix and enhanced collagen crosslinking [16]. This biological basis supports the reliability of elastography in differentiating malignant from benign calcifications, as demonstrated by the high AUC value (0.95) achieved in our study. Of note, our proposed cutoff of 62 kPa is consistent with prior literature, including the study by Chamming's et al. [17] which suggested a threshold of 64 kPa for Emean when evaluating breast microcalcifications. The similar cutoff range underscores the reproducibility of shear wave elastography metrics in diverse populations. However, minor differences in patient selection, imaging protocols, and

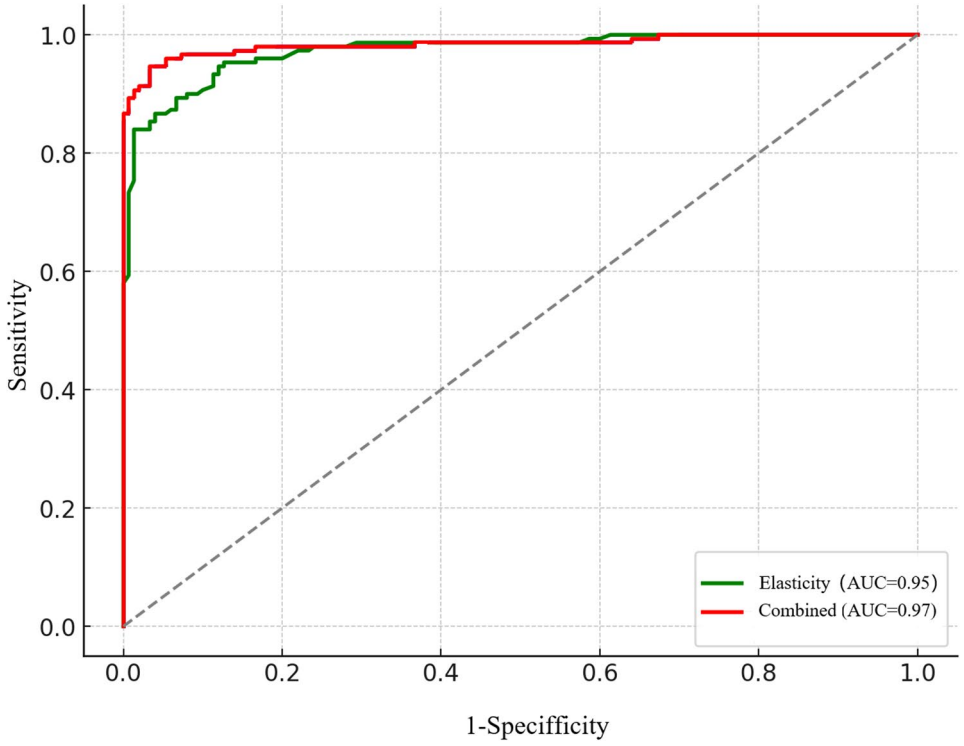

Fig. 4 Receiver operating characteristic (ROC) curves for different diagnostic models

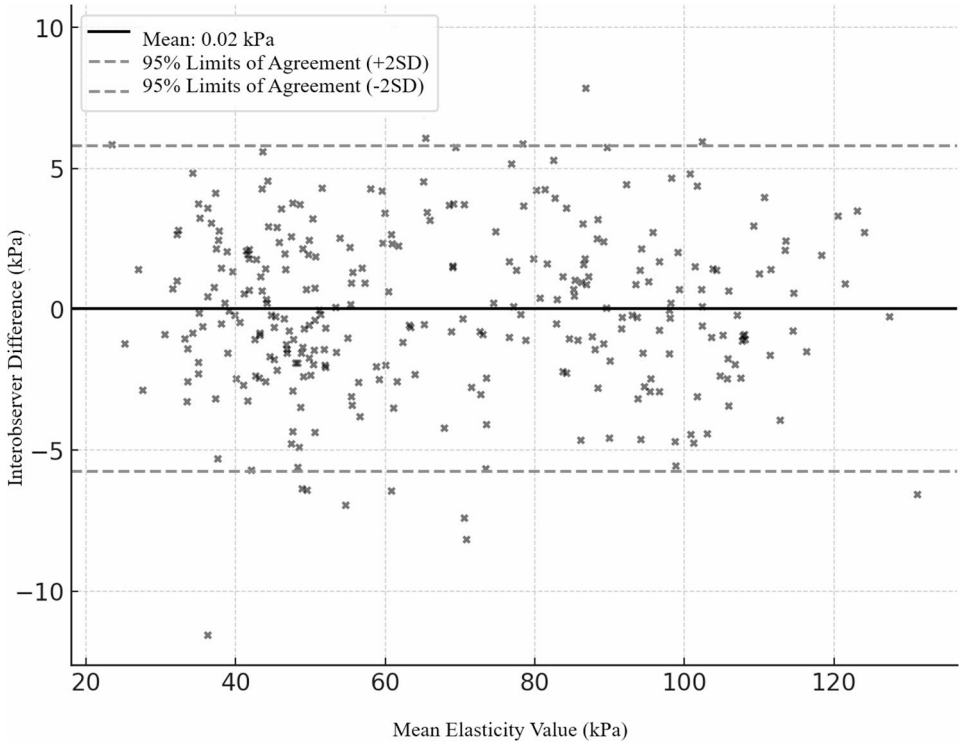

Fig. 5 Bland-altman plot of interobserver agreement

operator experience may lead to slight variations in the optimal cutoffs. Clinicians should exercise caution, particularly because a single cutoff value may not capture the complexities of all breast lesions and might require integration with conventional imaging and clinical judgment.The strong correlation between elasticity values and strain ratios ($r = 0.75$, $P < 0.001$) observed in our study suggests a robust relationship between different elastographic parameters. This finding is consistent with recent multi-center studies that have demonstrated the complementary nature of various elastographic measurements in breast lesion characterization [18]. The improvement in AUC from 0.95 to 0.97 when combining these parameters underscores the value of a multi-parameter approach, as supported by recent machine learning applications in breast imaging [19].

Our finding that elastography maintains good discriminatory power across different breast density categories is particularly noteworthy. Recent studies have highlighted the challenges of conventional imaging in dense breast tissue [20]. The optimal cutoff value of 62 kPa identified in our study achieved high sensitivity (88.0%) and specificity (86.7%), comparing favorably with recent meta-analyses of elastography in breast lesion characterization [21]. We acknowledge that a sensitivity of 88% could mean missing up to 12% of malignant lesions if 62 kPa were used as a strict "no-biopsy" cutoff. In clinical practice, other suspicious features on mammography or ultrasound, as well as patient risk factors, would still prompt further investigation even if the elastography reading is below this threshold. Thus, our proposed value should be seen as an adjunct rather than a replacement for standard diagnostic pathways.

The high interobserver agreement (Kappa = 0.84) demonstrated in our study addresses a critical concern in imaging biomarker validation. Recent standardization efforts in elastography have emphasized the importance of reproducible measurements [22], and our results support the reliability of this technique when performed following standardized protocols. The Bland-Altman analysis further confirms the measurement stability, with most variations falling within clinically acceptable limits.The multivariate analysis revealed that both elasticity value (OR = 1.09) and strain ratio (OR = 2.50) were independent predictors of malignancy, even after adjusting for conventional risk factors. This independence from traditional parameters suggests that elastography provides complementary diagnostic information, aligning with recent findings on the added value of functional imaging in breast diagnostics [23].

Our observation of elevated elastographic parameters in both ductal carcinoma in situ and invasive cancers suggests the technique's sensitivity to early-stage malignant changes. Recent molecular studies have shown that alterations in tissue mechanics occur early in the carcinogenic process [24], supporting the biological basis for elastography's diagnostic capability in early-stage disease. The high diagnostic accuracy achieved in our study may be particularly valuable in reducing unnecessary biopsies. With current positive predictive values for breast biopsies ranging from 20 to 30% [25], the addition of elastography could potentially improve patient selection for invasive procedures. The high negative predictive value in our study suggests particular utility in identifying benign lesions that might safely avoid biopsy.

Several limitations of our study warrant consideration. First, the case-control design may have introduced selection bias, potentially overestimating diagnostic accuracy compared to a prospective screening setting. Second, the single-center nature of the study and the use of specific ultrasound equipment may limit the generalizability of our findings. Third, the study focused on microcalcifications visible on ultrasound, potentially missing lesions only detectable on mammography. Fourth, the learning curve associated with elastography technique and interpretation was not specifically addressed in this study. Additionally, the influence of lesion depth and chest wall proximity on elastography measurements could not be fully controlled.

In conclusion, ultrasound elastography demonstrates high diagnostic accuracy in differentiating malignant from benign breast microcalcifications. The combination of quantitative elasticity values and strain ratios provides superior performance compared to single parameters alone, and our findings align with previous research suggesting cutoffs around 60–64 kPa. Although further large-scale, multi-center studies are needed, these results support elastography's potential utility as a valuable adjunct in the clinical evaluation of breast microcalcifications, possibly reducing unnecessary biopsies and expediting interventions in truly malignant cases.

Author contributions

JY and SSF were involved in the conception and design, or analysis and interpretation of the data; JY, SSF the drafting of the paper, revising it critically for intellectual content; JY the final approval of the version to be published; and that all authors agree to be accountable for all aspects of the work.

Funding

No funding was received.

Data availability

The datasets used and/or analyzed during the current study are available from the corresponding author on reasonable request.

Declarations

Ethical approval

The study was approved by the Ethics Committee of Hunan Provincial People's Hospital(HN-CS-2023-035).

Consent for publication

All authors confirm their consent to publication.

Clinical trial number
Not applicable.

Competing interests
The authors declare no competing interests.

Author details
[1]Department of Ultrasound Medicine, Hunan Provincial People's Hospital, First Affiliated Hospital of Hunan Normal University, Changsha, Hunan Province 410002, China
[2]General emergency department, Hunan Children's Hospital, Changsha, Hunan Province 410001, China
[3]No. 61, jiefang West Road, Furong District, Changsha City, Hunan Province 410002, China

Received: 24 December 2024 / Accepted: 17 March 2025
Published online: 24 April 2025

References

1. Bray F, Laversanne M, Weiderpass E, et al. The ever-increasing importance of cancer as a leading cause of premature death worldwide. Cancer. 2021;127(16):3029–30.
2. Cai G, Guo Y, Chen W, et al. Computer-aided detection and diagnosis of microcalcification clusters on full field digital mammograms based on deep learning method using neutrosophic boosting. Multimedia Tools Appl. 2020;79:17147–67.
3. Mann RM, Cho N, Moy L. Breast MRI: state of the art. Radiology. 2019;292(3):520–36.
4. Azam S, Eriksson M, Sjölander A, et al. Mammographic microcalcifications and risk of breast cancer. Br J Cancer. 2021;125(5):759–65.
5. Berg WA, Mendelson EB, Cosgrove DO, et al. Quantitative maximum shear-wave stiffness of breast masses as a predictor of histopathologic severity. Am J Roentgenol. 2015;205(2):448–55.
6. Pillai A, Voruganti T, Barr R, et al. Diagnostic accuracy of shear-wave elastography for breast lesion characterization in women: a systematic review and meta-analysis. J Am Coll Radiol. 2022;19(5):625–e6340.
7. Cantisani V, David E, Barr RG, et al. US-elastography for breast lesion characterization: prospective comparison of US BIRADS, strain elastography and shear wave elastography. Ultraschall Med. 2021;42(05):533–40.
8. Kim MY, Kim SY, Kim YS, et al. Added value of deep learning-based computer-aided diagnosis and shear wave elastography to b-mode ultrasound for evaluation of breast masses detected by screening ultrasound. Medicine. 2021;100(31):e26823.
9. Cantisani V, David E, Barr RG, et al. US-Elastography for Breast Lesion Characterization: Prospective Comparison of US BIRADS, Strain Elastography and Shear wave Elastography. US-Elastografie zur Charakterisierung von Brustläsionen: Prospektiver Vergleich von US-BI-RADS, Strain-Elastografie und Scherwellen-Elastografie. Ultraschall Med. 2021;42(5):533–40.
10. Kanagaraju V, Dhivya B, Devanand B, et al. Utility of ultrasound strain elastography to differentiate benign from malignant lesions of the breast. J Med Ultrasound. 2021;29(2):89–93.
11. Gu J, Jiang T. Ultrasound radiomics in personalized breast management: Current status and future prospects. Front Oncol. 2022;12:963612.
12. Cè M, D'Amico NC, Danesini GM, et al. Ultrasound elastography: basic principles and examples of clinical applications with artificial intelligence—a review. BioMedInformatics. 2023;3(1):17–43.
13. Safdar NM, Banja JD, Meltzer CC. Ethical considerations in artificial intelligence. Eur J Radiol. 2020;122:108768.
14. Karalis VD. The integration of artificial intelligence into clinical practice. Appl Biosci. 2024;3(1):14–44.
15. Garzotto F, Comoretto RI, Michieletto S, et al. Preoperative non-palpable breast lesion localization, innovative techniques and clinical outcomes in surgical practice: A systematic review and meta-analysis. Breast. 2021;58:93–105.
16. Golemati S, Cokkinos DD. Recent advances in vascular ultrasound imaging technology and their clinical implications. Ultrasonics. 2022;119:106599.
17. Chamming's F, Mesurolle B, Antonescu R, et al. Value of shear wave elastography for the differentiation of benign and malignant microcalcifications of the breast. AJR Am J Roentgenol. 2019;213(2):W85–92.
18. Sivarajah RT, Brown K, Chetlen A. I can see clearly now. Fundamentals of breast ultrasound optimization. Clin Imaging. 2020;64:124–35.
19. Li H, Bhatt M, Qu Z, et al. Deep learning in ultrasound elastography imaging: A review. Med Phys. 2022;49(9):5993–6018.
20. Bodewes FTH, Van Asselt AA, Dorrius MD, et al. Mammographic breast density and the risk of breast cancer: A systematic review and meta-analysis. Breast. 2022;66:62–8.
21. Deeg J, Swoboda M, Egle D, et al. Shear-wave elastography gradient analysis of newly diagnosed breast tumours: a critical analysis. Diagnostics. 2024;14(15):1657.
22. Santiago T, Santos E, Ruaro B, et al. Ultrasound and elastography in the assessment of skin involvement in systemic sclerosis: a systematic literature review focusing on validation and standardization–WSF Skin Ultrasound Group. Semin Arthritis Rheum. 2022;52:151954.
23. Ventura C, Baldassarre S, Cerimele F, et al. 2D shear wave elastography in evaluation of prognostic factors in breast cancer. Radiol Med. 2022;127(11):1221–7.
24. Mancini A, Gentile MT, Pentimalli F, et al. Multiple aspects of matrix stiffness in cancer progression. Front Oncol. 2024;14:1406644.
25. Lee CI, Abraham L, Miglioretti DL, et al. National performance benchmarks for screening digital breast tomosynthesis: update from the Breast Cancer Surveillance Consortium. Radiology. 2023;307(4):e222499.

Publisher's note